Field Emission of a Single In-Doped ZnO Nanowire

ARTICLE *in* THE JOURNAL OF PHYSICAL CHEMISTRY C · JUNE 2007

Impact Factor: 4.77 · DOI: 10.1021/jp0666030

ARTICLES

Field Emission of a Single In-Doped ZnO Nanowire

Yunhua Huang,[†] Yue Zhang,*[,†,§] Yousong Gu,[†] Xuedong Bai,[‡] Junjie Qi,[†] Qingliang Liao,[†] and Juan Liu[†]

Department of Materials Physics, University of Science and Technology Beijing, Beijing 100083, China, State Key Laboratory for Surface Physics, Institute of Physics, Chinese Academy of Sciences, Beijing 100080, China, and State Key Laboratory for Advanced Metals and Materials, University of Science and Technology Beijing, Beijing 100083, China

Received: October 8, 2006; In Final Form: May 3, 2007

In-doped ZnO nanowires were successfully fabricated by thermal evaporation of a powder mixture of Zn, In_2O_3, and graphite. Field emission of individual In-doped and pure ZnO nanowire was observed in situ by a transmission electron microscopy. The results show that In-doped ZnO nanowires showed an enhanced field emission properties. First-principle density functional calculations were performed to calculate the electronic structure of the In-doped and pure ZnO in order to explain the observed field emission properties. A two-band field emission mechanics was proposed to explain the enhanced field emission from n-type doping.

1. Introduction

Recently, many research efforts have been invested in the area of wide band gap semiconductor materials due to their wide range of applications. Among them, ZnO is an II−VI compound semiconductor with a wide and direct band gap of 3.3 eV and large exciton binding energy(60meV). Due to the superior conducting properties due to oxygen vacancies, ZnO has been investigated as a transparent conducting and piezoelectric materials in solar cells, electrodes, and sensors.[1−9] For applications in UV light emitters, varistors, piezoelectric transducer, chemical and gas sensing, transparent high-power electronic, and surface acoustic wave devices, ZnO was frequently doped with Ga, In, Sn, and Al to enhance the electrical, optical, and magnetic properties.[10−17] So far, besides the physical properties of one-dimensional (1D) doped ZnO nanostructures, field emission (FE) properties of mass pure and Ga-doped 1D ZnO nanostructures have been reported.[18−21] To given materials, FE properties are mainly dependent on the morphology, dimension, and apex geometry of one-dimensional nanomaterials, and such researches have been reported.[21] Besides external causation, the internal or intrinsical feature are crucial to the FE properties of materials. For practical application in FE and relative area, investigation on intrinsical FE properties of individual and doped ZnO nanomaterials is indispensable.

In this paper, In-doped ZnO nanowires have been fabricated, and the field emission properties of single In-doped ZnO nanowire have been studied. Density functional calculations were performed to explain the enhanced field emission, and a two-band model was proposed to explain field emissions from n-type materials.

2. Method Section

The In-doped ZnO nanowires were synthsized through the mixture of zinc (99.9%purity, 50 μm in size), In_2O_3 (99.9%purity, 50 μm in size), and graphite (99.9%purity, 40 μm in size) powders with the mole ratio of 3:1:2 in an Al_2O_3 boat inside a quartz tube at 930 °C, and the silicon substrate was coated with catalytic Au nanoparticles prepared from $HAuCl_4 \cdot 3H_2O$ (98%, from Sigma) ethanol solution. Ar was used as the carrier gas and O_2 the reaction gas. The flow rate of Ar and O_2 was about 250−350 and 5−10 standard cm^3 min^{-1} (sccm), respectively. The morphologies and structures of the products were investigated by field-emission scanning electron microscopy (FESEM)(LEO1530), X-ray diffractometer (XRD) (D8 Discover with Co target and GADDS). Field emission measurement was performed on a special setup inside a JEOL-2010 FEG TEM.

Density functional calculations were performed to calculate the electronic structure of theoretical pure ZnO, ZnO with oxygen vacancy, and In-doped ZnO in order to study the intrinsical field emission properties. PAW pseudo-potential and PBE exchange correlation functional were employed in the calculations. Coulomb interaction between the d electrons was included in a LDA+U scheme in order to treat the strong correlation between d electrons in ZnO, and the U value is 5.0 and 7.0 eV for In and Zn respectively. K-point density is 50 A, and energy cut off is 400 eV. Oxygen deficiency was assumed to be 1/16, i.e., $Zn_{16}O_{15}$. Doping was realized by construct a 2 × 2 × 2 supercell and replace one Zn ion with In. Geometry

* Corresponding author. Tel.: +86-10-62333113. Fax: +86-10-62332281. E-mail address: Yuezhang@ustb.edu.cn.

† Department of Materials Physics, University of Science and Technology Beijing.

‡ Chinese Academy of Sciences.

§ State Key Laboratory for Advanced Metals and Materials, University of Science and Technology Beijing.

10.1021/jp0666030 CCC: $37.00
Published on Web 06/05/2007

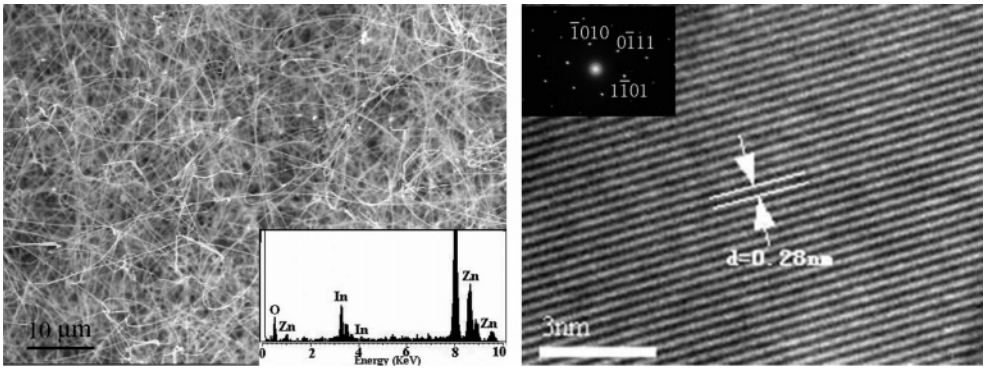

Figure 1. (a) SEM image of In-doped ZnO nanowires grown on the golden particle coated Si substrate. The EDX data shows 17.2 atom % In (inset). (b) HRTEM image of the nanowire. The inset is the corresponding SEAD pattern.

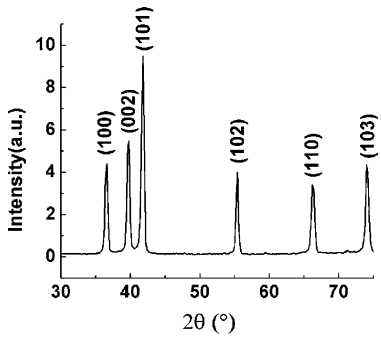

Figure 2. XRD pattern taken from the In-doped ZnO nanowires.

relations were performed for both the lattice and internal atomic position before the ground state electronic structures were calculated.

3. Results and Discussion

In-doped ZnO nanowires were shown in Figure 1. The nanowires have the diameters in the range of 30−100 nm, and average length of about 20 μm. EDX in Figure 1a confirms that the composition of the nanowires is Zn, O, and In, and the In content is about 17.2 atom %. Figure 1b shows the HRTEM image and the corresponding SEAD pattern of the nanowire. XRD pattern of the nanowires are shown in Figure 2. The diffraction peaks were indexed to hexagonal wurtzite structure, and indicated that the products were In-doped ZnO with single phase. Fabrication and structural characterization of pure ZnO nanowires were reported in our previous article.[22]

For in situ TEM measurement and imaging, a special TEM specimen holder was built for a JEOL 2010 FEG TEM operated under the vacuum of 10^{-7} Torr and at room temperature. An electrochemically etched tungsten needle served as the movable cathode, its opposite gold wire was the anode. The gold wire was melted as ball shape at end. The distance between two electrodes can be precisely controlled by the piezo-manipulator. The individual pure and In-doped ZnO nanowires were fixed on the tungsten tip by using graphite paste. The schematic frame is shown in Figure 3a. The TEM beam was blank out during field emission measurement and the nanowire was discharged in advance. Figure 3b,c shows the pure and In-doped ZnO nanowires used for field emission measurement, and the dimension and apex geometry of the nanowires are on the same scale. The interelectrode distances for FE measuring are 1.5 μm.

The measured results are shown in Figure 4 for both the In-doped and pure ZnO nanowires. Due to the thermal vibration and deflexion induced by voltage changes, the nanowires, especially the tips swayed accordingly in the measurement, and then the obtained data of emission current presented mild fluctuation. According to the definition (turn-on voltage was defined as the voltage required to generate a current of 0.1 μA) and the data, the turn-on voltage for a single nanowire is found to be about 342 and 290 V for pure and In-doped ZnO, and the corresponding turn-on field is 228 and 193 V/μm, respectively. For the block materials and the mass nanomaterials such as the nanoarrays, the emission current I is actually the emission current density, its unit is A/cm^2, and the turn-on voltage/field is the voltage/field that generates a current density of 0.1 μA/cm^2. The current density of 0.1 μA/cm^2 at the turn-on field (about several V/μm) of ZnO nanoarray is contributed by the great numbers of nanowires at 1 cm^2,[18−21] whereas the current of 0.1 μA at the turn-on field (228 V/μm and 193 V/μm) in the present experiments is contributed by a single pure or In-doped ZnO nanowire respectively. Compared with single emission, the individual nanowire in arrays needs a much higher field to generate a given current because of the interference effect. In other words, for an individual nanowire, the turn-on field in single wire measuring is much lower than that in mass wires measuring.

On the basis of the above, In-doped ZnO nanowire shows a turn-on voltage much lower than that of pure ZnO nanowire. The emission current of the pure nanowire increases exponentially as the interelectrode voltage increase and reaches 0.73 μA at 420 V, while that of In-doped nanowire show a more complex fashion, and reaches 1.27 μA at 420 V. A two-step increasing mode is clearly visible for the later one. It is obviously that the performance of field emission from the individual In-doped ZnO nanowire is better than that of the single pure ZnO nanowire.

The field emission current follows the Folwer−Nordheim-(FN) model. In the F−N theory, the field emission current is determined by two factors: field enhancement factor β and work function φ, which is expressed as

$$I = KF^2/\varphi \exp(-B\varphi^{3/2}/F) \qquad (1)$$

where $B = 6.83 \times 103$ eV^{-3}/2 V μm^{-1} and K is a constant. The local electric field F is usually related to the applied voltage V as $F = \beta V/d$, where β is the field enhancement factor and V/d is the average field.

The F−N plot [ln(I/V^2) versus 1/V] is used to study its characteristics. It can be approximately fitted to a straight line,

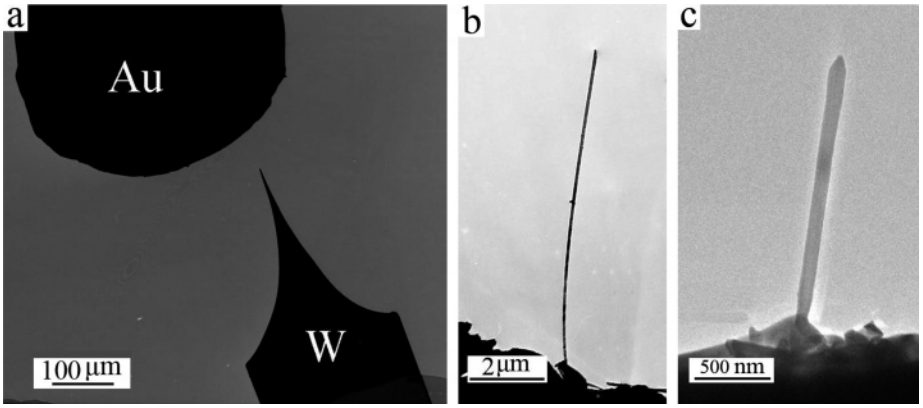

Figure 3. (a) Setup of the in situ measurement. (b) A single ZnO nanowire with a diameter of approximately 100 nm and (c) pure In-doped ZnO nanowire with a diameter of approximately 100 nm used in field emission measurement.

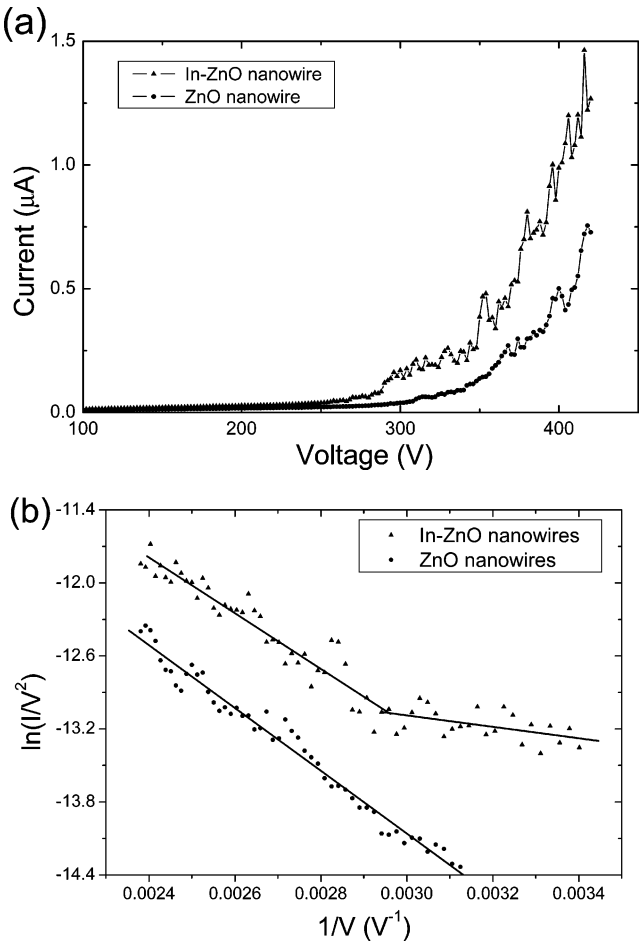

Figure 4. (a) $I-V$ curves and (b) the corresponding F−N plots for a single In-doped ZnO nanowire and ZnO nanowire, respectively. The lines in the F−N plots are the linear fit of the experimental curves.

where the slope k can by expressed as

$$k = -B\varphi^{3/2}\mathrm{d}/\beta \qquad (2)$$

Figure 4b shows the F−N plot. The F−N plot of pure naoowire can be easily fitted into a straight line, while that of In-doped nanowire can be fitted to two straight line, corresponding to the two step mode in the $I-V$ curve. For undoped ZnO nanowire, the slope is estimated 2582 V by assuming a work function value of φ =5.3 eV for ZnO; the field enhancement factor β is calculated to be 48.4. Since the geometry used for field emission measurement is the same for both the pure and In-doped ZnO nanowires, the field enahncement factor β was assume to be the same. From the two slope values of 2290 and 470 V, we calculated the work function of In-doped ZnO to be 4.89 and 1.70 eV, with an energy difference of 3.19 eV. This value is nearly equal to the band gap of ZnO. From the above estimation, we can see that the In-doped ZnO have a small work function value as compared to the pure ZnO. The conduction band participate in electron emission, since In-doped ZnO is an n-type semiconductor, the work function is further decreased to as low as 1.70 eV.

TABLE 1: Band Structure Properties of ZnO (Unit: eV)

	d band	d ban width	p band	p band width	band gap (Eg)
pure ZnO	−9.09 to −7.93	1.16	−3.98 to −0.03	3.95	2.80
ZnO with O vacancy	−9.02 to −7.14	1.88	−5.88 to −0.96	4.92	1.56
In−ZnO	−10.32 to −8.77	1.55	−7.63 to −2.67	4.96	1.24

Density functional calculation were performed to calculate the electronic structures of In doped ZnO, and the density of state (DOS) for theoretical pure ZnO, ZnO with O vacancy, and In-doped ZnO were calculated. Figure shows the overall DOS and detailed DOS near the Fermi level. It can be seen that pure ZnO is an intrinsic semiconductor with a band gap of 2.8 eV, while In-doped ZnO is an n-type semiconductor. The detailed results of band structure are shown in Table 1. For pure ZnO, the band gap is Eg = 2.80 eV, a little bit smaller than the experimental value of 3.3 eV. This is quite usual in first-principle calculations and much better than the calculation without taking into account the Coulomb interaction. For ZnO with O vacancy and In-doped ZnO (6.25 at. %), the bandwidth become narrow due to donor levels.

Two-step field emission behavior of In-doped ZnO nanowire can be explained with the calculated band structure. After doping with In, ZnO become an n-type semiconductor, with the Fermi level lying at the bottom of the conduction band. The electrons participated in the field emission comes from two parts: the deep valence band and the part of conduction band below the Fermi level. The emission current from the conduction band has a small work function (measured from the Fermilevel to vacuum state), so the turn-on voltage is low. However, since the density of state is quite low, the emission current is small and is insignificant when the emission from valence band is dominant as the

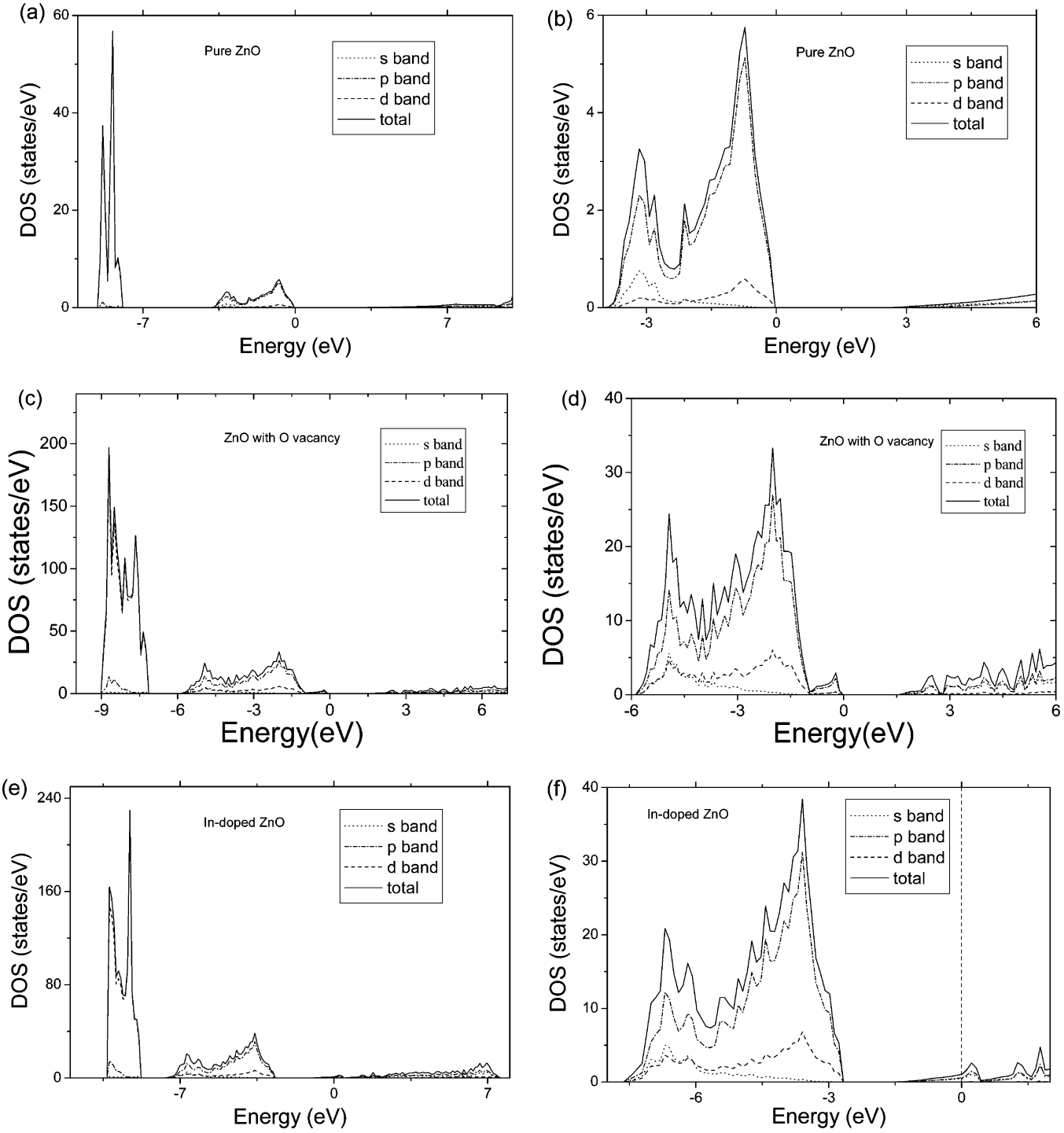

Figure 5. DOS of pure ZnO, ZnO with O vacancy, and In-doped ZnO calculated by density functional theory. Overall DOS of (a) pure ZnO, (c) ZnO with O vacancy, (e) In-doped ZnO, (b) pure ZnO, (d) ZnO with O vacancy, and (f) In-doped ZnO.

applied voltage is increased. For the valence band, the work function is measured from the top of valence band to vacuum, and it is −2.67 eV larger than that of the conduction band. The difference is quite close to the measured value of 3.19 eV.

Since experimental undoped ZnO nanowires are often oxygen deficient, band structures of ZnO with oxygen deficiency are calculated. By comparing the DOS plot of pure and oxygen deficient ZnO, it can be seen that the later is n-type semiconductor, with the donor level just above the valence band. For field emission, it will behave as the pure ZnO, with a little bit smaller work functions.

4. Conclusions

Pure and In-doped ZnO nanowires were successfully fabricated by thermal evaporation, and the field emission properties have been investigated in situ by a transmission electron microscopy. The results show that In-doped ZnO nanowires showed a two step field emission mode and enhanced field emission property. First-principle density functional calculations were performed to calculate the electronic structure of pure and In-doped ZnO in order to explain the observed field emission properties. A two-band field emission mechanics was proposed to explain the observed field emission from n-type doping.

Acknowledgment. This work was supported by the National Science Fund for Distinguished Young Scholars (No. 50325209), the National High Technology Research and Development Program of China (No. 2006AA03Z351), and the Major Project of International Cooperation and Exchanges (No. 50620120439, 2006DFB51000).

References and Notes

(1) Pan, Z.; Dai, Z.; Wang, Z. L. *Science* **2001**, *291*, 1947.
(2) Xia, Y.; Yang, P.; Sun, Y.; Wu, Y.; Mayers, B.; Gates, B.; Yin, Y.; Kim, F.; Yan, H. *Adv. Mater.* **2003**, *15*, 353.
(3) Kong, X. Y.; Wang, Z. L. *Nano Lett.* **2003**, *3*, 1625.
(4) Zhao, M. H.; Wang, Z. L.; Mao, S. X. *Nano Lett.* **2004**, *4*, 587.
(5) Hughes, W. L.; Wang, Z. L. *J. Am. Chem. Soc.* **2004**, *126*, 6703.
(6) Wan, Q.; Li, Q. H.; Chen, Y. J.; Wang, T. H. *Appl. Phys. Lett.* **2004**, *84*, 3654.
(7) Wang, Z. L.; Kong, X. Y.; Ding, Y.; Gao, P. X.; Hughes, W. L.; Yang, R.; Zhang, Y. *Adv. Funct. Mater.* **2004**, *14*, 943.
(8) Özgür, Ü.; Alivov, Y. I.; Liu, C.; Teke, A.; Reshchikov, M. A.; Doğan, S.; Avrutin, V. C. S. J.; Morkoçd, H. *J. Appl. Phys.* **2005**, *98*, 041301.
(9) Patolsky, F.; Lieber, C. M. *Mater. Today* **2005**, *8*, 20.
(10) Ren, C. Y.; Chiou, S. H.; Hsue, C. S. *Phys. B* **2004**, *349*, 136.
(11) Jie, J. S.; Wang, G. Z.; Han, X. H. *Chem. Phys. Lett.* **2004**, *387*, 466.
(12) Bae, S. Y.; Na, C. W.; Kang, J. H.; Park, J. *J. Phys. Chem. B* **2005**, *109*, 2526.
(13) Bae, S. Y.; Choi, H. C.; Na, C. W.; Park. J. H. *Appl. Phys. Lett.* **2005**, *86*, 0331021.
(14) Liu, J.; Zhang, Y.; Qi, J.; Huang, Y.; Zhang, X.; Liao, Q. *Mater. Lett.* **2006**, *60*, 2623.
(15) Roy, V. A. L.; Djurisic, A. B.; Liu, H.; Zhang, X. X.; Leung, Y. H.; Xie, M. H.; Gao, J.; Lui, H. F.; Surya, C. *Appl. Phys. Lett.* **2004**, *84*, 756.
(16) Shan, F. K.; Yu, Y. S. *J. Euro. Ceram.* **2004**, *24*, 1869.
(17) Yamamoto, T.; Sakemi, T.; Awai, K.; Shirakata, S. *Thin Solid Films* **2004**, *451*, 439.
(18) Lee, C. J.; Lee, T. J.; Lyu, S. C.; Zhang, Y. *Appl. Phys. Lett.* **2002**, *81*, 3648.
(19) Zhu, Y. W.; Zhang, H. Z.; Sun, X. C.; Feng, S. Q.; Xu, J.; Zhao, Q.; Xiang, B.; Wang, R. M.; Yu, D. P. *Appl. Phys. Lett.* **2003**, *83*, 144.
(20) Xu, C. X.; Sun, X. W.; Chen, B. *J. Appl. Phys. Lett.* **2004**, *84*, 1540.
(21) Huang, Y. H.; Zhang, Y.; Liu, L.; Fan, S. S.; Wei, Y.; He, J. J. *Nanosci. Nanotechnol.* **2006**, *6*, 787.
(22) Huang, Y.; Bai, X.; Zhang, Y. *J. Phys.: Condens. Matter* **2006**, *18*, L179.